

Canopy1, a positive feedback regulator of FGF signaling, controls progenitor cell clustering during Kupffer's vesicle organogenesis

Takaaki Matsui^{a,1}, Siripong Thitamadee^{a,2}, Tomoko Murata^a, Hisaya Kakinuma^b, Takuji Nabetani^c, Yoshio Hirabayashi^c, Yoshikazu Hirate^d, Hitoshi Okamoto^b, and Yasumasa Bessho^a

^aGene Regulation Research, Graduate School of Biological Sciences, Nara Institute of Science and Technology, 8916-5 Takayama, Nara 630-0101, Japan; ^bLaboratory for Developmental Gene Regulation, and ^cHirabayashi Research Unit, Brain Science Institute, RIKEN, 2-1 Hirosawa, Wako, Saitama 351-0198, Japan; and ^dDepartment of Cell Fate Control, Institute of Molecular Embryology and Genetics, Kumamoto University, 2-2-1 Honjo, Kumamoto 860-0811, Japan

Edited by Igor B. Dawid, National Institute of Child Health and Human Development, Bethesda, MD, and approved May 10, 2011 (received for review November 18, 2010)

The assembly of progenitor cells is a crucial step for organ formation during vertebrate development. Kupffer's vesicle (KV), a key organ required for the left–right asymmetric body plan in zebrafish, is generated from a cluster of ~20 dorsal forerunner cells (DFCs). Although several genes are known to be involved in KV formation, how DFC clustering is regulated and how cluster formation then contributes to KV formation remain unclear. Here we show that positive feedback regulation of FGF signaling by Canopy1 (Cnpy1) controls DFC clustering. Cnpy1 positively regulates FGF signals within DFCs, which in turn promote Cadherin1-mediated cell adhesion between adjacent DFCs to sustain cell cluster formation. When this FGF positive feedback loop is disrupted, the DFC cluster fails to form, eventually leading to KV malformation and defects in the establishment of laterality. Our results therefore uncover both a previously unidentified role of FGF signaling during vertebrate organogenesis and a regulatory mechanism underlying cell cluster formation, which is an indispensable step for formation of a functional KV and establishment of the left–right asymmetric body plan.

left–right patterning | ciliogenesis

Fibroblast growth factor (FGF) signaling plays crucial roles in multiple morphogenetic processes of vertebrate development, including gastrulation movement, mesoderm formation, and left–right (LR) patterning (1–3). Because gain or loss of function of FGF signaling results in morphological changes in the embryo, some mechanism must ensure appropriate FGF signal levels in space and time for proper morphogenesis throughout development. FGF effectors acting as positive or negative regulators show a wide range of expression patterns and activities, contributing to the precise regulation of FGF signal activity (1, 4). Although most effectors identified to date act as negative regulators of FGF signaling, a few that positively regulate FGF activity have been reported (1, 4).

We recently identified in zebrafish a positive regulator of FGF signaling named *canopy1* (*cnpy1*), which is required for maintenance of the midbrain–hindbrain boundary (MHB) (5). Expression of *cnpy1* was restricted to the MHB at late-somitogenesis stages, whereas *cnpy1* was broadly distributed in earlier embryos (5) (*SI Appendix, Fig. S1A*), suggesting an additional role(s) for Cnpy1-mediated FGF signaling beyond the regulation of MHB formation. In this study, we characterize *cnpy1* in detail during early zebrafish development and show that a Cnpy1-mediated positive feedback loop of FGF signaling promotes cell cluster formation between dorsal forerunner cells (DFCs) during gastrulation. We also demonstrate that the failure of DFCs to cluster when this FGF positive loop is disrupted eventually leads to Kupffer's vesicle (KV) malformation and randomization of LR asymmetric patterning.

Results

Positive Feedback Loop of FGF Signaling Mediated by Cnpy1 Is Activated Specifically in DFCs During Zebrafish Gastrulation.

To reveal the role of Cnpy1-mediated FGF signaling in early zebrafish embryos, we first looked for the specific regions and cells in which Cnpy1 positively regulates FGF signaling, by monitoring FGF signal activity using an anti-di-phosphorylated Erk (dp-Erk) antibody. FGF signal activity was observed in the blastoderm margin and DFCs at midgastrulation (*SI Appendix, Fig. S2A*), whereas knockdown of *cnpy1* with an antisense morpholino (*cnpy1*-MO) reduced the FGF activity in DFCs (*SI Appendix, Fig. S2B*). To test whether Cnpy1 is required autonomously for the FGF activation in DFCs, we next knocked down *cnpy1* in DFCs but not in the rest of the embryo by using a DFC-specific MO delivery method (6–8). Similar to *cnpy1* morphants, DFC-specific knockdown of *cnpy1* (DFC^{*cnpy1*-MO}) reduced the FGF activity in DFCs (Fig. 1*B* and *SI Appendix, Fig. S2C*). Because *cnpy1* expression is induced by Fgf8 in the MHB (5), we checked whether FGF signaling is also required for *cnpy1* expression in DFCs. We found that *cnpy1* expression in DFCs could indeed be blocked by knockdown of *fgf8* (*SI Appendix, Fig. S2G*) or by treatment with the FGF receptor inhibitor SU5402 (Fig. 1*D*). These results imply that a positive feedback loop between FGF and Cnpy1 is activated specifically in DFCs at midgastrulation.

Cnpy1 Function Within DFCs Is Required for DFC Clustering.

DFCs are progenitor cells of KV, which is a key organ required for LR patterning (9–11). At midgastrulation, a cluster of ~20 DFCs appears adjacent to the embryonic shield (12, 13). The DFC cluster then moves to the vegetal pole and forms a more compact and oval-shaped cluster by late gastrulation (7, 11, 14). At the end of gastrulation, DFCs differentiate into ciliated epithelial cells of the KV, which generates the nodal flow required for LR patterning (7, 12, 13). Recent studies have shown that FGF signaling is required for morphogenesis and ciliogenesis of the KV as well as for LR patterning (2, 8, 15). Although knockdown of the FGF target genes *ier2* and *fbp1* is known to interfere with

Author contributions: T. Matsui and Y.B. designed research; T. Matsui, T. Murata, H.K., and T.N. performed research; Y. Hirate and H.O. contributed new reagents/analytic tools; T. Matsui, S.T., H.K., T.N., Y. Hirabayashi, and H.O. analyzed data; and T. Matsui and S.T. wrote the paper.

The authors declare no conflict of interest.

This article is a PNAS Direct Submission.

¹To whom correspondence should be addressed. E-mail: matsui@bs.naist.jp.

²Present address: Department of Biotechnology, Faculty of Science, Mahidol University, Ratchathewi, Bangkok 10400, Thailand.

This article contains supporting information online at www.pnas.org/lookup/suppl/doi:10.1073/pnas.1017248108/-DCSupplemental.

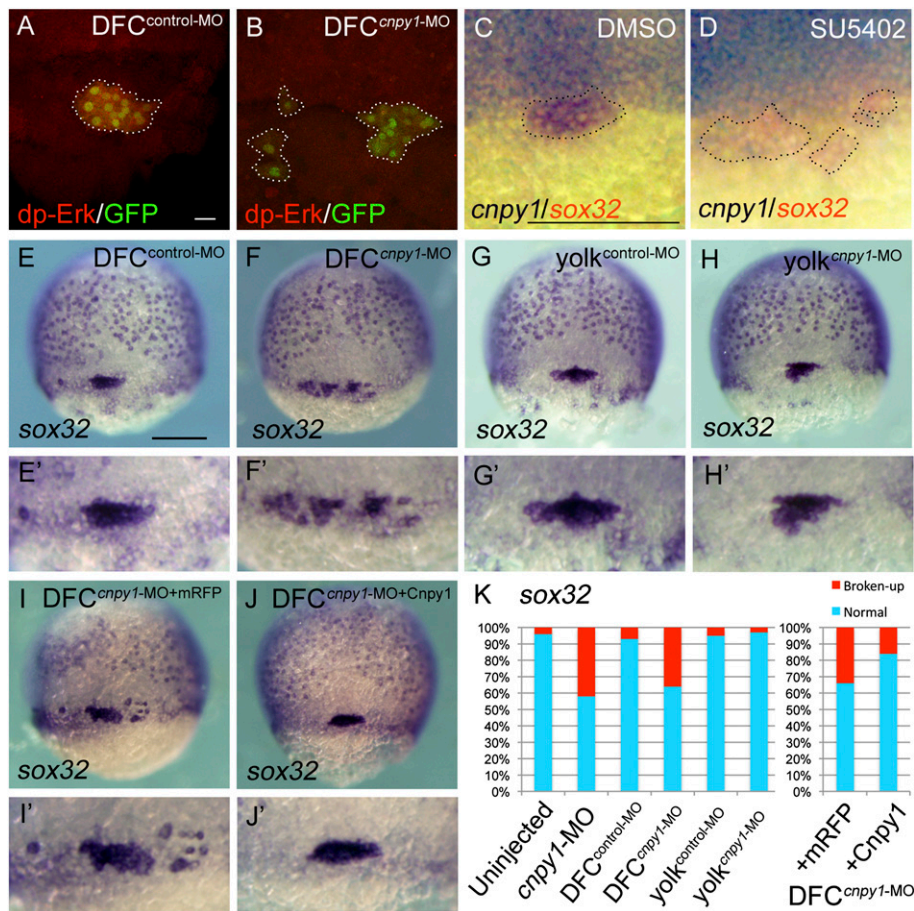


Fig. 1. *Cnpy1* within DFCs regulates DFC clustering. (A and B) dp-Erk staining in DFC^{control-MO}-injected (A) or DFC^{*cnp1*-MO}-injected (B) *Tg[sox17:GFP]* embryos at 60% epiboly stage. (Scale bar: 20 μ m.) dp-Erk signals (red) were down-regulated in GFP-positive DFCs (green). (C and D) *cnp1* (purple) and *sox32* (red) expression in DMSO-treated (C) or SU5402-treated (D) embryos at 60% epiboly stage. (Scale bar: 200 μ m.) Dotted lines in A–D mark the outlines of DFC populations. (E–J) *sox32* expression in DFC^{control-MO} (E), DFC^{*cnp1*-MO} (F), *yolk*^{control-MO} (G), *yolk*^{*cnp1*-MO} (H), DFC^{*cnp1*-MO+mRFP} (I), or DFC^{*cnp1*-MO+Cnpy1} (J) embryos at 70% epiboly stage. Dorsal view, anterior to the top. (Scale bar: 200 μ m.) (E'–J') Higher-magnification images highlight DFCs. (K) Percentages of normal (clustered) or broken-up DFCs were scored by using the *sox32* expression pattern in uninjected ($n = 68$), *cnp1*-MO ($n = 77$), DFC^{control-MO} ($n = 61$), DFC^{*cnp1*-MO} ($n = 78$), *yolk*^{control-MO} ($n = 56$), *yolk*^{*cnp1*-MO} ($n = 62$), DFC^{*cnp1*-MO+mRFP} ($n = 119$), or DFC^{*cnp1*-MO+Cnpy1} ($n = 123$) embryos. Statistically significant ($P < 0.05$) differences could be seen in uninjected versus *cnp1*-MO, DFC^{control-MO} versus DFC^{*cnp1*-MO}, and DFC^{*cnp1*-MO+mRFP} versus DFC^{*cnp1*-MO+Cnpy1} embryos.

DFC formation (15), the contribution of FGF signaling before KV formation is poorly understood.

To investigate the role of *Cnpy1* in DFC/KV formation, we analyzed the expression of markers specific for DFC fate specification (*sox32*) or differentiation (*no tail*) in *cnp1*-MO-injected embryos. We found that the DFC cluster was broken up into multiple groups of cells (Fig. 1K and *SI Appendix*, Fig. S3B, C, and E), and the broad distribution of endoderm cells marked by *sox32* was disrupted (*SI Appendix*, Fig. S3B) in *cnp1* morphants. Even though *cnp1* morphants showed a failure of DFC clustering, neither cell fate specification nor total cell number in DFCs was affected by *cnp1* knockdown (*SI Appendix*, Fig. S3B and Table S1). Similar to *cnp1* morphants, DFC-specific knockdown of *cnp1* resulted in a broken-up DFC phenotype, whereas DFC specification and cell number were unaffected (Fig. 1F and K and *SI Appendix*, Fig. S3C and G and Table S1). When embryos were coinjected with *cnp1*-MO and MO-resistant *cnp1* mRNA (DFC^{*cnp1*-MO+Cnpy1}), the broken-up DFC phenotype was significantly rescued (53%; $P = 0.00174$; Fig. 1I–K). Because, in the DFC-specific MO delivery method, the MO is also delivered to the yolk and the yolk syncytial layer (YSL), it was possible that effects of *cnp1* in yolk/YSL might be essential for DFC clustering. To address this, we knocked down *cnp1* in yolk/YSL but not

in DFCs (*yolk*^{*cnp1*-MO}) and found no DFC defects in terms of specification, cell number, or cluster formation (Fig. 1H and K and *SI Appendix*, Table S1). Live confocal imaging revealed that the sparse DFC populations in DFC^{*cnp1*-MO} embryos never assembled into a compact cluster, although normal downward migration was observed (*SI Appendix*, Fig. S4 and *Movies S1* and *S2*), indicating that *Cnpy1* regulates formation of the cell cluster itself, rather than controlling directed cell migration.

***Cnpy1* Function Within DFCs Is Essential for KV Ciliogenesis and LR Patterning.**

Observation of DFCs using zebrafish embryos from transgenic line *Tg[sox17:GFP]* revealed that broken-up DFC phenotypes did not generate multiple clusters at the end of gastrulation. In DFC^{*cnp1*-MO}-injected embryos, a rosette-like structure containing a small number of DFCs was formed, around which fragmented GFP signals that might signify dead cells could be observed, whereas a proper rosette structure containing a larger number of DFCs was evident in DFC^{control-MO} embryos (*SI Appendix*, Fig. S5C–E). These results suggest that the broken-up DFC clusters seen in DFC^{*cnp1*-MO} embryos reflect a failure in the recruitment of DFCs to the KV.

To examine how the failure of DFC cluster formation influences KV organogenesis and function, we investigated the presence and characteristics of primary cilia in the KV in DFC^{*cnp1*-MO} mor-

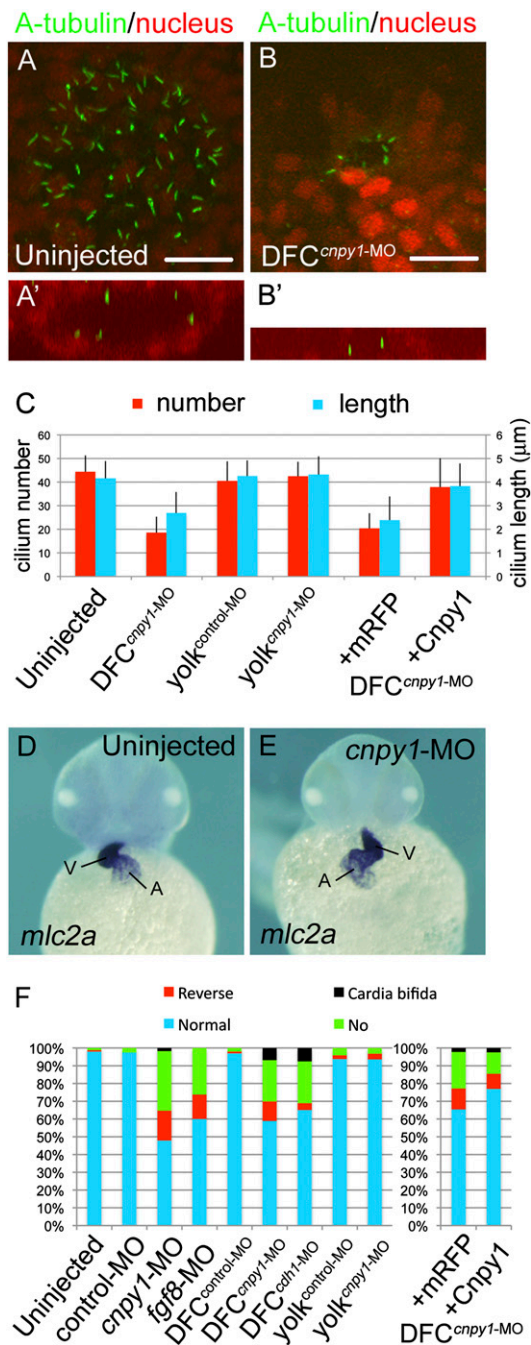


Fig. 2. *Cnpy1* function within DFCs is essential for ciliogenesis and LR patterning. (A and B) A-tubulin (green) and nucleus (red) staining in uninjected (A) or DFC^{cnpy1-MO}-injected (B) embryos at the six-somite stage. Vegetal pole view. (Scale bars: 20 μ m.) (A' and B') X-Z view around the KV. Lumen formation was not completed in DFC^{cnpy1-MO}-injected embryos (B'). (C) Number (red) or length (blue) of KV primary cilia in uninjected ($n = 10$ or 49), DFC^{cnpy1-MO} ($n = 10$ or 48), *yolk*^{control-MO} ($n = 11$ or 77), *yolk*^{cnpy1-MO} ($n = 11$ or 58), DFC^{cnpy1-MO+mRFP} ($n = 10$ or 61), or DFC^{cnpy1-MO+Cnpy1} ($n = 11$ or 85) embryos. (Error bars show SEM.) Statistically significant ($P < 0.05$) differences could be seen in uninjected versus DFC^{cnpy1-MO} and DFC^{cnpy1-MO+mRFP} versus DFC^{cnpy1-MO+Cnpy1} embryos. (D and E) Representative images of *mlc2a* expression demonstrating normal looping (uninjected; D) or reversed looping (*cnpy1-MO*; E) of the heart in embryos at the high pec stage. Ventral view, anterior to the top. A, atrium; V, ventricle. (F) Percentages of normal looping, reversed looping, no looping, or cardia bifida of the heart in uninjected ($n = 164$), control-MO ($n = 118$), *cnpy1-MO* ($n = 119$), *fgf8-MO* ($n = 65$), DFC^{control-MO} ($n = 95$), DFC^{cnpy1-MO} ($n = 146$), DFC^{cdh1-MO} ($n = 106$), *yolk*^{control-MO} ($n = 96$), *yolk*^{cnpy1-MO} ($n = 94$), DFC^{cnpy1-MO+mRFP} ($n = 136$), and

phants by using an anti-acetylated tubulin (A-tubulin) antibody. DFC-specific knockdown of *cnpy1* resulted in 60% and 35% reductions in the number and length, respectively, of primary cilia in the KV at early somitogenesis (Fig. 2 B and C). In addition to this disruption of ciliogenesis, lumen formation in the KV was incomplete (Fig. 2B'), suggesting that *Cnpy1*-mediated DFC clustering is required for proper formation of the KV. This idea is supported by the observation that the horseshoe-shaped pattern of *charon* expression in the caudal region of the KV was lost in DFC^{cnpy1-MO} morphants (SI Appendix, Fig. S6 B and C). Consistent with these defects, knockdown of *cnpy1* altered the left-sided expression of *southpaw* (*spaw*) in the lateral plate mesoderm at late somitogenesis (SI Appendix, Fig. S6 E and F) and led to defects in cardiac laterality at later stages (Fig. 2 E and F). Defective ciliogenesis and cardiac laterality in DFC^{cnpy1-MO} embryos could be rescued by coinjection of MO-resistant *cnpy1* mRNA (Fig. 2C and SI Appendix, Fig. S7D). Collectively, these results suggest essential roles for *cnpy1* in KV ciliogenesis and LR patterning.

Amplification of FGF Signaling by *Cnpy1* Is Required for DFC Clustering. The above phenotypes in DFC^{cnpy1-MO} embryos are reminiscent of the defects seen in embryos in which FGF signaling has been disrupted, such as *fgf8*, *fgfr1*, *ier2*, and *fibp1* morphants (Fig. 2F and SI Appendix, Fig. S6F) (8, 15). To test for a functional relationship between FGF signaling and *cnpy1* in DFC clustering, we analyzed whether the loss of FGF signaling function could phenocopy *cnpy1* morphants. Intriguingly, *ace1/fgf8* mutations lead to failures of KV formation and LR patterning (2). Although *fgf8* is expressed in and around DFCs (2), overlapping with *cnpy1* expression, the role of *fgf8* in DFC clustering is uncertain. We therefore examined the contribution of *fgf8* to the formation of the DFC cluster. As for *cnpy1-MO*-injected embryos, *fgf8* morphants exhibited the broken-up DFC phenotype (Fig. 3 A-C and SI Appendix, Table S1). *fgf8* knockdown also resulted in defects in KV formation (SI Appendix, Fig. S6C) and LR patterning (Fig. 2F and SI Appendix, Fig. S6F). We also found that 57% of the *ace1/fgf8* mutants displayed the broken-up DFC phenotype (SI Appendix, Fig. S8 C and D). These results suggest that *fgf8* plays an essential role in DFC clustering and that *Cnpy1* contributes to this role.

We have shown that *Cnpy1* is a protein localized to the endoplasmic reticulum (ER) that can interact with *Fgfr1* (5). However, it is still unclear how *Cnpy1* modulates FGF signaling. Because the ER is a quality-control system that ensures maturation of secreted and membrane-bound proteins (16, 17), we reasoned that *Cnpy1* might assist in the maturation of *Fgfr1* in the ER, and we tested this with *in vitro* glycosylation assays (SI Appendix, Materials and Methods). Mature forms of *Fgfr1* increased up to twofold in *Cnpy1*-overexpressing cells (Fig. 4 A and B), suggesting that *Cnpy1* enhances FGF signaling by promoting the maturation of its receptor in the ER. This idea was further supported by proteomic data showing that a human *Cnpy1* homolog binds to ER chaperones and folding-assisting enzymes (SI Appendix, Table S2).

If the amplification of FGF signals via *Cnpy1*-mediated *Fgfr1* maturation is required for DFC clustering, it seemed possible that forced activation of *Fgfr1* would restore the failure of DFC clustering in DFC^{cnpy1-MO} embryos. Using iFGFR1, a conditional activation system for *Fgfr1* that depends on AP20187-induced dimerization (5, 18), we activated *Fgfr1* spatially and temporally in DFCs (SI Appendix, Materials and Methods). AP20187-mediated conditional activation of *Fgfr1* in DFCs led to a 67% reduction in the broken-up DFC phenotype relative to vehicle (ethanol)-

DFC^{cnpy1-MO+Cnpy1} ($n = 165$) embryos. Statistically significant ($P < 0.05$) differences could be seen in uninjected versus *cnpy1-MO*, DFC^{control-MO} versus DFC^{cnpy1-MO}, and DFC^{cnpy1-MO+mRFP} versus DFC^{cnpy1-MO+Cnpy1} embryos.

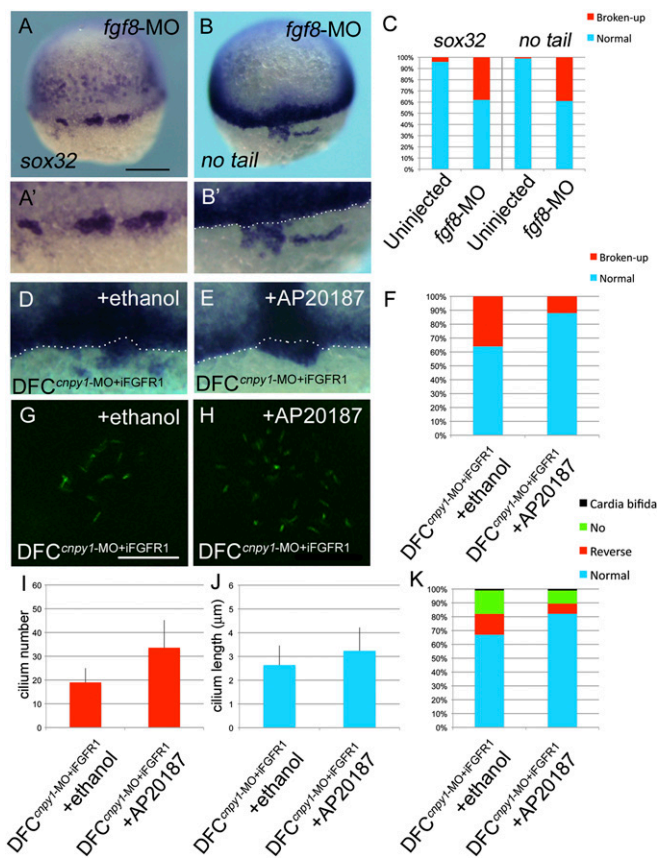


Fig. 3. FGF signaling plays crucial roles in DFC clustering and KV ciliogenesis. (A and B) *sox32* (A) or *no tail* (B) expression in *fgf8*-MO-injected embryos. Dorsal view, anterior to the top. (Scale bar: 200 μ m.) (A' and B') Higher-magnification images highlight DFCs. (B', D, and E) The white dotted lines mark the boundary between DFCs and the blastoderm margin. (C) Percentages of normal or broken-up DFCs were scored by using the *sox32* or *no tail* expression patterns in uninjected ($n = 68$ or 89) or *fgf8*-MO ($n = 61$ or 69) embryos. Statistically significant ($P < 0.05$) differences could be seen in uninjected versus *fgf8*-MO embryos. (D–F) Transient activation of FGF signaling restored the broken-up DFC phenotype (D–F), ciliogenesis (G–J), and cardiac laterality (K) in *DFC^{cnpy1-MO+IFGFR1}* embryos. (D and E) Expression of *no tail* in *DFC^{cnpy1-MO+IFGFR1}* embryos treated with ethanol (D) or AP20187 (E). (F) Percentages of broken-up DFC phenotype in ethanol-treated ($n = 84$) or AP20187-treated ($n = 93$) *DFC^{cnpy1-MO+IFGFR1}* embryos. The conditional activation of Fgfr1 after treatment with AP20187 significantly decreased the broken-up DFC phenotype (67%; $P < 0.05$) (G–J) A-tubulin (green) staining in ethanol-treated (G) or AP20187-treated (H) *DFC^{cnpy1-MO+IFGFR1}* embryos at the six-somite stage. (Scale bar: 20 μ m.) (I and J) Number (I) or length (J) of KV primary cilia in ethanol-treated *DFC^{cnpy1-MO+IFGFR1}* ($n = 9$ or 36) or AP20187-treated *DFC^{cnpy1-MO+IFGFR1}* ($n = 8$ or 34) embryos at the six-somite stage. (Error bars show SEM.) Statistically significant ($P < 0.05$) differences could be seen in ethanol-treated versus AP20187-treated *DFC^{cnpy1-MO+IFGFR1}* embryos. (K) Percentages of cardiac laterality defect in ethanol-treated ($n = 89$) or AP20187-treated ($n = 102$) *DFC^{cnpy1-MO+IFGFR1}* embryos. The conditional activation of Fgfr1 after treatment with AP20187 alleviated the cardiac laterality defect (48%; $P < 0.05$).

treated controls ($P = 2.89 \times 10^{-4}$; Fig. 3 D–F). Despite the conditional activation being restricted to DFCs during gastrulation, this manipulation partially restored deficiencies in cilium number ($P = 9.23 \times 10^{-3}$) and length ($P = 7.77 \times 10^{-3}$) in the KV (Fig. 3 G–J) and in cardiac laterality at later stages ($P = 0.0114$; Fig. 3K). These results therefore indicate that Cnpy1 function reinforces FGF signal activity within DFCs and suggest that DFC clustering mediated by this positive loop is a prerequisite for formation of a functional KV and proper LR patterning.

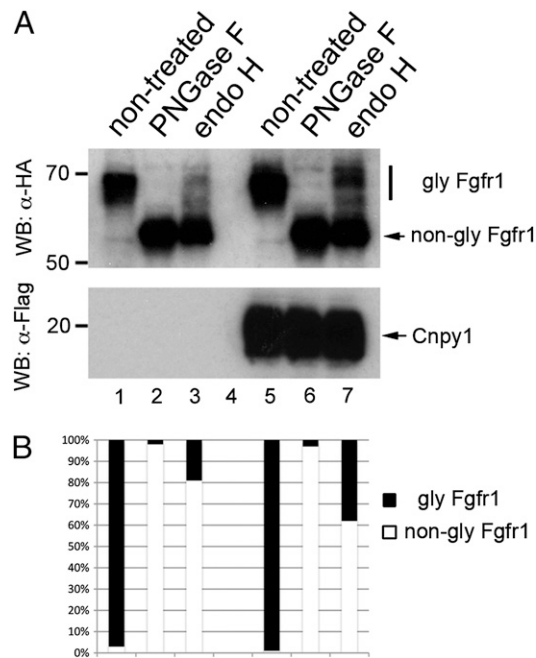


Fig. 4. Cnpy1 enhances FGF receptor maturation within the ER. (A and B) Fgfr1 N-glycosylation level was examined by PNGase F (lanes 2 and 6) or endo H (lanes 3 and 7) treatment. Lanes 1–3, mock control cells; lanes 5–7, Cnpy1-overexpressing cells. Fgfr1 and Cnpy1 were tagged with HA and Flag, respectively (SI Appendix, Materials and Methods). Upper indicates the glycosylation levels of Fgfr1, and Lower shows expression of Cnpy1 protein. (B) Ratio of glycosylated (black) and nonglycosylated (white) forms of Fgfr1. The amount of the endo H-resistant mature form of Fgfr1 in Cnpy1-overexpressing cells (lane 7) was twice that in mock control cells (lane 3).

Induction of *cadherin1* (*cdh1*) by Cnpy1-Mediated FGF Signaling Is Responsible for Generating Cell Adhesion Between DFCs.

To investigate the cellular function of Cnpy1 in DFC clustering, we analyzed cytoskeletal organization in DFCs of *DFC^{cnpy1-MO}* embryos. Phalloidin staining showed that F-actin accumulated to a high level at the cell–cell contact sites between DFCs containing control-MO (SI Appendix, Fig. S9A), meaning that DFCs adhered tightly to each other in control embryos. In contrast, cell–cell adhesion between DFCs containing *cnpy1*-MO, evaluated by F-actin accumulation, was weaker than that between control-MO-containing DFCs (SI Appendix, Fig. S9B). These results suggest that Cnpy1-mediated FGF signaling modulates cell adhesions between DFCs during the control of cell clustering.

Recent studies have shown that the T-box transcription factor Tbx16 regulates DFC/KV formation in a cell-autonomous manner, although the underlying mechanism is still unclear (7). Tbx16 is also a mediator of FGF signaling, a function that is implicated in the control of cell adhesions via the transcriptional regulation of *paraxial protocadherin* (*papc*) (7, 19). Although *papc* expression is not detected in DFCs, *cdh1* expression is (7, 20); thus, we hypothesized that *tbx16* and *cdh1* are downstream effectors of FGF signaling during the control of DFC clustering. To test this possibility, we analyzed whether Cnpy1-mediated FGF signaling affects expression of *tbx16* or *cdh1* within DFCs. *DFC^{cnpy1-MO}* embryos showed reduced *tbx16* or *cdh1* expression in sparse DFC populations (Fig. 5 B and D and SI Appendix, Fig. S10 B and D). Importantly, DFC-specific knockdown of *tbx16* (*DFC^{tbx16-MO}*) also led to a reduction of *cdh1* expression within DFCs (SI Appendix, Fig. S10 E and G), suggesting that *tbx16* plays an important role in *cdh1* expression within DFCs.

We next investigated whether DFC-specific knockdown of *tbx16* (*DFC^{tbx16-MO}*) or *cdh1* (*DFC^{cdh1-MO}*) could phenocopy

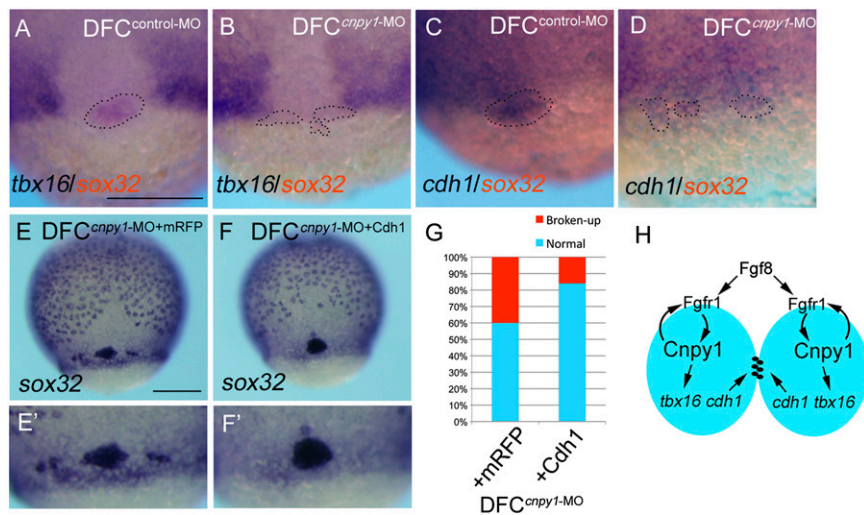


Fig. 5. A Cnpy1-mediated FGF positive loop regulates cell adhesion through the control of *cdh1* expression. (A and B) *cdh1* (purple) and *sox32* (red) expression in DFC^{control-MO} (A) or DFC^{Cnpy1-MO} (B) embryos at 65% epiboly stage. (C and D) *tbx16* (purple) and *sox32* (red) expression in DFC^{control-MO} (C) or DFC^{Cnpy1-MO} (D) embryos at 65% epiboly stage. Dotted lines in A–D mark the outlines of DFC populations. (Scale bar: 200 μ m.) (E and F) Expression of *sox32* in DFC^{Cnpy1-MO}+mRFP (E) or DFC^{Cnpy1-MO}+*Cdh1* (F) embryos at 80% epiboly. (Scale bar: 200 μ m.) (G) Percentage of broken-up DFC phenotype in mRFP-overexpressing ($n = 82$) or *Cdh1*-overexpressing ($n = 103$) DFC^{Cnpy1-MO} embryos. Overexpression of *Cdh1* rescued the broken-up DFC phenotype in DFC^{Cnpy1-MO} embryos (60%; $P < 0.05$). (H) Diagram illustrating the FGF-dependent cell–cell communication control mechanisms of the forerunner cell cluster during early development. The model depicts the activation of intracellular FGF signaling via binding of Fgf8 ligands and Fgfr1 on the cell surface of two adjacent DFCs (blue ovals). The amplified FGF signal, through Cnpy1-mediated maturation of Fgfr1 within DFCs, subsequently activates the expression of *tbx16* and *cdh1* to organize forerunner cells as a cluster.

DFC^{Cnpy1-MO} morphants. DFC-specific knockdown of either *tbx16* or *cdh1* led to the broken-up DFC phenotype (SI Appendix, Fig. S11 B–D and Table S1), outcomes similar to those observed in DFC^{Cnpy1-MO} morphants. These results suggested that a genetic cascade including *tbx16* and *cdh1* mediates FGF signal-dependent DFC clustering and prompted us to examine whether the broken-up DFC phenotype in DFC^{Cnpy1-MO} embryos could be rescued by overexpressing *Cdh1*. This restored DFC clustering in 60% of the manipulated embryos, relative to overexpression of monomeric red fluorescent protein (mRFP) as a control (Fig. 5 E–G). Hence, our results demonstrate that the Cnpy1-mediated FGF positive feedback loop regulates *tbx16* and *cdh1* to assemble cells into a tight cluster.

Taking into account all of these results, we propose the following stepwise regulatory mechanism underlying DFC cluster formation (Fig. 5H). First, FGF signaling is initiated in DFCs by Fgf8. Second, the up-regulated Cnpy1 within DFCs modulates FGF signal strength by enhancing Fgfr1 maturation in the ER. Third, the amplified FGF signals then promote cell–cell adhesion between adjacent DFCs through the action of *Cdh1*, eventually leading to the generation of a tight and stable cluster of DFCs.

Discussion

Accumulated evidence points to crucial roles of FGF signaling in several processes of LR asymmetric patterning (2, 8, 9, 15, 21, 22). Two recent studies, in particular, have shown that FGF signaling regulates KV ciliogenesis during LR patterning (8, 15). However, we uncover the importance of this signal pathway for the regulation of progenitor cell clustering at a stage before KV ciliogenesis: DFC-specific knockdown of *cnp1*, *tbx16*, or *cdh1* results in broken-up DFC clusters during gastrulation. The cause of such a discrepancy may originate from the differences of regulatory mechanisms underlying DFC cluster formation and ciliogenesis. DFC clustering requires activities of FGF-dependent effectors such as *tbx16* and *cdh1*, as shown in this study. In contrast, ciliogenesis depends on the intraflagellar transport pathway

regulated by the coordinated action of various signals, including FGF, Sonic hedgehog, and/or Wnt pathways (8, 15, 23, 24).

In this study, we have proposed that Cnpy1 controls DFC clustering, KV formation, and ciliogenesis by promoting Fgfr1 maturation. However, Neugebauer et al. (8) showed a different and specific role of *fgfr1* in ciliogenesis and KV formation: DFC-specific knockdown of *fgfr1* (DFC^{fgfr1-MO}) leads to short cilia without affecting cilium number and KV size. This discrepancy may explain the redundant action between *fgfr1* paralogs. A recent study has shown that the *fgfr1* that was knocked down by Neugebauer et al. (8) and a second *fgfr1* (*fgfr1b*) can functionally compensate for each other during early development (25). We reasoned that DFC-specific knockdown of *cnp1* might lead to defects more severe than those seen in DFC^{fgfr1-MO} embryos because Cnpy1 can modulate the maturation of both receptors within DFCs. To test this possibility, we used a dominant-negative form of Fgfr1 (dn-Fgfr1), which lacks the cytoplasmic domain, and attempted to inhibit the functions of both receptors. Because injection of *dn-fgfr1* mRNA into one-cell embryos led to severe defects in mesoderm formation and axis elongation, as shown previously (1), we used DFC-specific gene-transfer methods. As seen in DFC^{Cnpy1-MO} embryos, DFC^{dn-Fgfr1} embryos resulted in a broken-up DFC phenotype (SI Appendix, Fig. S12 B and C). Treatment with SU5402 (100 μ g/mL) also led to broken-up DFC clusters (Fig. 1D). These results therefore suggest that strong loss-of-function effects on Fgfr1, such as *cnp1* knockdown, dn-Fgfr1 overexpression, and SU5402 treatment, prevent DFCs from organizing into a tight cell cluster, and that Cnpy1 may assist the maturation of both receptors within DFCs. On the other hand, mild loss of Fgfr1 function, including the single knockdown of *fgfr1* performed by Neugebauer et al. (8), may yield the specific defect in cilium length.

Our results do not support data showing that loss of FGF signaling function—by SU5402 treatment (6–7 μ g/mL), genetic disruption of *fgf8* and/or *fgf24*, or ectopic expression of dn-Fgfr1 using *hsp70:dn-fgfr1* transgenic zebrafish—leads to a specific defect in cilium length (8). This discrepancy may arise from variable loss-of-function efficiency caused by different inhibitor concen-

trations, genetic backgrounds, or experimental protocols. Regarding the role of *fgf8* in LR asymmetry, severe KV defects—including partial or complete loss of KV formation, short cilia, and a reduced number of cilia—have been observed in *ace/fgf8* mutants or knockdown embryos of *fgf8* or *fgf8* effectors (*ier2* and *fibp1*) (2, 15). In addition, Hong and Dawid (15) have reported that severe KV defects in knockdown embryos of *ier2* and *fibp1* may be associated with disorganization of the DFC cluster. These findings also differ from those of Neugebauer et al. (8) but are consistent with our observations that either *ace/fgf8* mutants or *fgf8* morphants display failures of DFC clustering, KV formation, and LR patterning. Although particular issues remain to be resolved, these results clearly demonstrate that FGF signaling plays important roles in DFC clustering, KV formation, and ciliogenesis.

Contact between DFCs and the overlying surface ectoderm is known to be important for DFCs to migrate toward the vegetal pole (14). Because loss of function of FGF signal components (*fgf8* and *cnpy1*) and downstream effectors (*tbx16* and *cdh1*) showed the broken-up DFC clusters but normal migration of these disrupted DFCs to the vegetal pole during gastrulation, FGF signal-dependent cell adhesion may specifically contribute to the interaction among DFCs themselves. However, in these phenotypes, some DFCs remained capable of interacting with others to form small groups of cells, implying that other factor(s) may contribute to DFC clustering. It has been reported that integrin αV and integrin $\beta 1b$ have a role in DFC clustering (26) and that planar cell polarity signaling regulates cell adhesion between DFCs (27). Additional experiments to clarify the relationship between FGF signaling and integrins or planar cell polarity signaling during DFC cluster formation will be important to understand the entire mechanism underlying DFC cluster formation.

Conclusions

We have discovered the cells (DFCs) in which *Cnpy1* functions and further added an insight into the molecular mechanism by which *Cnpy1* regulates cell signaling in the ER. We identified an essential signal cascade—ligand, receptor, mediator, and downstream effector—that is required for proper cluster formation by progenitor cells. In addition, our findings reveal that progenitor clustering regulated by a positive feedback loop of cell signaling contributes to the formation of a functional organ to establish the LR asymmetric body plan during vertebrate development.

Materials and Methods

Zebrafish and Whole-Mount in Situ Hybridization. A wild-type strain (RIKEN-Wako), *Tg[sox17:GFP]* (28), and *ace^{ti282a}* (2) were used in this study. Single- or double-color whole-mount in situ hybridization was performed as described previously (29, 30). cDNA fragments of *cdh1*, *cnpy1*, *mlc2a*, *no tail*, *sox32*, and *spaw* were used as templates for the antisense probes.

Other Methods. Detailed methods for immunofluorescence analyses, pharmacological experiments, and rescue experiments are available in *SI Appendix, Materials and Methods*.

ACKNOWLEDGMENTS. We are grateful to Thomas N. Sato, Yasukazu Nakahata, and Kinichi Nakashima for advice, helpful discussions, and critical reading of the manuscript. We also thank Ian Smith for help in preparing the manuscript; Ryutaro Akiyama, Maiko Yokouchi, Takeshi Fujimuro, and Naoyuki Tahara for technical assistance; Tatsuro Matsuta for help with statistical analysis; Bruce W. Draper for advice; Kazushige Sakaguchi, Masahiko Hibi, and Masatoshi Takeichi for sharing reagents; Kota Yanagitani, Michiko Saito, and Kenji Kohno for sharing reagents and discussions; National BioResource Project Zebrafish, Core Institution for zebrafish lines *Tg[sox17:GFP]* and *ace^{ti282a}*, and ARIAD for AP20187. This work was supported by Grants-in-Aid for Scientific Research on Priority Areas “WAKATE (B)” and “Systems Genomics” from the Ministry of Education, Culture, Sports, Science, and Technology (MEXT), Japan; the Nakajima Foundation; and the Global Center of Excellence Program of Nara Institute of Science and Technology, MEXT, Japan.

- Böttcher RT, Niehrs C (2005) Fibroblast growth factor signaling during early vertebrate development. *Endocr Rev* 26:63–77.
- Albertson RC, Yelick PC (2005) Roles for *fgf8* signaling in left–right patterning of the visceral organs and craniofacial skeleton. *Dev Biol* 283:310–321.
- Meyers EN, Martin GR (1999) Differences in left–right axis pathways in mouse and chick: Functions of FGF8 and SHH. *Science* 285:403–406.
- Tsang M, Dawid IB (2004) Promotion and attenuation of FGF signaling through the Ras-MAPK pathway. *Sci STKE* 2004:pe17.
- Hirate Y, Okamoto H (2006) Canopy1, a novel regulator of FGF signaling around the midbrain–hindbrain boundary in zebrafish. *Curr Biol* 16:421–427.
- Amack JD, Yost HJ (2004) The T box transcription factor no tail in ciliated cells controls zebrafish left–right asymmetry. *Curr Biol* 14:685–690.
- Amack JD, Wang X, Yost HJ (2007) Two T-box genes play independent and cooperative roles to regulate morphogenesis of ciliated Kupffer's vesicle in zebrafish. *Dev Biol* 310:196–210.
- Neugebauer JM, Amack JD, Peterson AG, Bisgrove BW, Yost HJ (2009) FGF signalling during embryo development regulates cilia length in diverse epithelia. *Nature* 458: 651–654.
- Hirokawa N, Tanaka Y, Okada Y, Takeda S (2006) Nodal flow and the generation of left–right asymmetry. *Cell* 125:33–45.
- Kramer-Zucker AG, et al. (2005) Cilia-driven fluid flow in the zebrafish pronephros, brain and Kupffer's vesicle is required for normal organogenesis. *Development* 132: 1907–1921.
- Essner JJ, Amack JD, Nyholm MK, Harris EB, Yost HJ (2005) Kupffer's vesicle is a ciliated organ of asymmetry in the zebrafish embryo that initiates left–right development of the brain, heart and gut. *Development* 132:1247–1260.
- Cooper MS, D'Amico LA (1996) A cluster of noninvoluting endocytic cells at the margin of the zebrafish blastoderm marks the site of embryonic shield formation. *Dev Biol* 180:184–198.
- Melby AE, Warga RM, Kimmel CB (1996) Specification of cell fates at the dorsal margin of the zebrafish gastrula. *Development* 122:2225–2237.
- Oteiza P, Köppen M, Concha ML, Heisenberg CP (2008) Origin and shaping of the laterality organ in zebrafish. *Development* 135:2807–2813.
- Hong SK, Dawid IB (2009) FGF-dependent left–right asymmetry patterning in zebrafish is mediated by *ier2* and *Fibp1*. *Proc Natl Acad Sci USA* 106:2230–2235.
- Sitia R, Braakman I (2003) Quality control in the endoplasmic reticulum protein factory. *Nature* 426:891–894.
- Wickner S, Maurizi MR, Gottesman S (1999) Posttranslational quality control: Folding, refolding, and degrading proteins. *Science* 286:1888–1893.
- Pownall ME, et al. (2003) An inducible system for the study of FGF signalling in early amphibian development. *Dev Biol* 256:89–99.
- Yamamoto A, et al. (1998) Zebrafish *paraxial protocadherin* is a downstream target of *spadetail* involved in morphogenesis of gastrula mesoderm. *Development* 125: 3389–3397.
- Esguerra CV, et al. (2007) Ttrap is an essential modulator of Smad3-dependent Nodal signaling during zebrafish gastrulation and left–right axis determination. *Development* 134:4381–4393.
- Hamada H, Meno C, Watanabe D, Saijoh Y (2002) Establishment of vertebrate left–right asymmetry. *Nat Rev Genet* 3:103–113.
- Raya A, Izpisua Belmonte JC (2006) Left–right asymmetry in the vertebrate embryo: From early information to higher-level integration. *Nat Rev Genet* 7:283–293.
- Eggenchwilier JT, Anderson KV (2007) Cilia and developmental signaling. *Annu Rev Cell Dev Biol* 23:345–373.
- Oishi I, Kawakami Y, Raya A, Callol-Massot C, Izpisua Belmonte JC (2006) Regulation of primary cilia formation and left–right patterning in zebrafish by a noncanonical Wnt signaling mediator, *duboraya*. *Nat Genet* 38:1316–1322.
- Rohner N, et al. (2009) Duplication of *fgfr1* permits Fgf signaling to serve as a target for selection during domestication. *Curr Biol* 19:1642–1647.
- Ablooglu AJ, Tkachenko E, Kang J, Shattil SJ (2010) Integrin αV is necessary for gastrulation movements that regulate vertebrate body asymmetry. *Development* 137:3449–3458.
- Oteiza P, et al. (2010) Planar cell polarity signalling regulates cell adhesion properties in progenitors of the zebrafish laterality organ. *Development* 137:3459–3468.
- Mizoguchi T, Verkade H, Heath JK, Kuroiwa A, Kikuchi Y (2008) *Sdf1/Cxcr4* signaling controls the dorsal migration of endodermal cells during zebrafish gastrulation. *Development* 135:2521–2529.
- Matsui T, et al. (2005) Noncanonical Wnt signaling regulates midline convergence of organ primordia during zebrafish development. *Genes Dev* 19:164–175.
- Hauptmann G, Gerster T (1994) Two-color whole-mount in situ hybridization to vertebrate and *Drosophila* embryos. *Trends Genet* 10:266.